

AntiBloom: A Novel Deep Learning-Powered Device to Predict Harmful Algal Blooms

Neel Bhattacharyya¹, Jay Wankhede¹ and Zachary Kingman[#]

¹Poolesville Highschool, USA

[#]Advisor

ABSTRACT

Harmful Algal Blooms (HABs) affect biosystems, leading to Unusual Marine Mortality Events (UMEs). Predicting algal bloom events can be costly and challenging. In this study, we developed a method for predicting algal blooms using an Artificial Neural Network (ANN) with Keras and Sklearn. We also designed a buoy that can collect real-time data on wind speed, UV index, pH, water temperature, and salinity to calculate real-time predictions of algal bloom. With a low cost of \$150, the buoy was equipped with imaging and notification capabilities using Amazon Web Services (AWS), enabling relevant parties to be informed of harmful conditions. The ANN was trained using data from the National Centers for Environmental Information, which provided water quality data sets for Lake Erie. The model demonstrated 96.34% accuracy in predicting elevated levels of chlorophyll-a, a common marker for detecting algae. The buoy and its algorithm significantly improve over current methods of detecting elevated chlorophyll-a levels, affirming their potential to be mass-produced and usable by local authorities.

Introduction

Algal blooms are an overgrowth of aquatic organisms that occur on the surface of lakes and other bodies of water in a short period of time. These blooms contain many species that can be harmful for various reasons, e.g., the production of toxins, hypoxia, and others. It has come to a point where this problem is widespread and growing and has negative consequences for aquatic ecosystems, human health, and the economy [1-4]. Algal blooms are most commonly attributed to an excess of nutrients (particularly phosphorus and nitrogen) and elevated temperatures [5, 6]. Other favorable conditions for algal blooms may include low wind speeds and prolonged storage of water [7-9]. The leading causes of water body eutrophication include runoff from agricultural fertilizer, livestock waste, sewage, and industrial waste products from surrounding activity [10].

As algae die and decompose, bacteria consume the remaining oxygen in the water, leading to hypoxic conditions that create "dead zones" where marine life cannot survive. The most detrimental algal blooms are caused by brown tide species (*Aureococcus anophagefferens* and *Aureoumbra lagunensis*), cyanobacteria, and dinoflagellates [11]. The algal blooms caused by cyanobacteria are prevalent and can have devastating impacts on aquatic life due to the release of cyanotoxins especially in fresh water. The brevetoxins produced by dinoflagellate *Karenia brevis*, one of the most common types of harmful algae blooms in the United States, can harm human and animal health, leading to various health issues and a full-blown water crisis [12]. Due to these issues, large lakes such as the Great Lakes have now been designated impaired under the Clean Water Act [13]. The incredible economic impacts of algal blooms are apparent all over the world as well. In the US, 4.6 billion dollars have been used for eutrophication-related remedies [14, 15]. Northeast Asia, Japan, and Korea have dealt with severe economic problems as well [16]. Previous literature analyzed the correlation between HABs with elevated temperature, total phosphorus, and nutrients [5,6,17-20]. Additionally, elevated levels of chlorophyll-a have an extremely high correlation with algal blooms, essentially making it an indicator of an oncoming

algal bloom which takes a minimum of five days to fully form [21]. Therefore, consistently predicting high levels of chlorophyll-a levels over some period of time would confirm the possibility of an incoming algal bloom. The chlorophyll-a concentrations proposed by the World Health Organization (WHO) are for low (< 10 $\mu\text{g/L}$), moderate (between 10 and 50 $\mu\text{g/L}$), high (between 50 and 5000 $\mu\text{g/L}$), and very high risk (>5000 $\mu\text{g/L}$) [22]. Yuan et al. demonstrated the strongest association of microcystin (one of the common toxins) with total nitrogen and chlorophyll-a [23]. These findings suggest that the concentration of chlorophyll-a could also be useful in tracking the new US Environmental Protection Agency (USEPA) microcystin health advisory levels for drinking water [24-26].

Machine learning has tremendous potential for predicting environmental disasters. With the help of large datasets, machine learning algorithms can accurately predict certain events based on parameters that have an effect. New research has shown that ANNs are highly effective for environmental event prediction [27]. This has prompted others to look at using machine learning to predict other natural disasters, such as tornadoes and wildfires [28, 29]. ANNs have also been proven to effectively combat nonlinearity and have been accurately used for ecological modeling in past research [29]. Previous studies have also used machine learning to predict algal blooms but have done so with parameters such as dissolved oxygen and satellite data [30]. These are attributes that are very expensive to use and are not feasible data points to collect for smaller ponds and lakes, which there are a lot more of. There is proper precedent and past research to support the possibility of using an ANN to predict elevated levels of chlorophyll-a effectively. To accurately predict the chlorophyll-a level for a body of water, a buoy can be used with sensors. Medina et al. developed a low-cost (\$658.79) buoy for remote water quality monitoring in fish farming [31]. They measure temperature, pH, and dissolved oxygen, transmitting the information locally through a low-power wide-area network protocol. Inspired by their results, we have developed the current, even lower-cost buoy (\$150) with the capability of predicting another important parameter, chlorophyll-a.

Materials and Methods

Development of Deep Learning Algorithm

The novel AntiBloom algorithm developed through an ANN using the Keras and Sklearn modules in Python was crafted to accurately predict chlorophyll-a levels. The hidden layers in an ANN are responsible for feature extraction, which identifies patterns in the input data. Each neuron in a hidden layer applies a non-linear activation function to the weighted sum of its inputs, allowing the network to learn complex relationships between the input features and the output variable. Our algorithm consisted of five attributes for each of the sensor readings, one hidden layer with four (number of attributes minus one) neurons, and an output layer with one neuron for the concentration of chlorophyll-a (Figure 1).

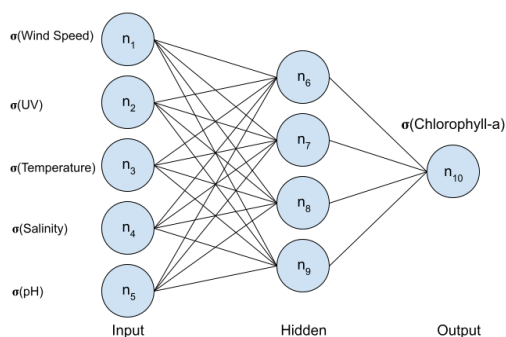


Figure 1. Representation of the Artificial Neural Network. Circles (attributes) represent neurons, and connections represent weights.

The values for each of the hidden layers and output layers are computed with the following equations.

$$f\left(\begin{bmatrix} w_{1,5} & w_{2,5} & w_{3,5} & w_{4,5} & w_{5,5} \\ w_{1,6} & w_{2,6} & w_{3,6} & w_{4,6} & w_{5,6} \\ w_{1,7} & w_{2,7} & w_{3,7} & w_{4,7} & w_{5,7} \\ w_{1,8} & w_{2,8} & w_{3,8} & w_{4,8} & w_{5,8} \end{bmatrix} \cdot \begin{bmatrix} n_1 \\ n_2 \\ n_3 \\ n_4 \\ n_5 \end{bmatrix} + \begin{bmatrix} b_6 \\ b_7 \\ b_8 \\ b_9 \end{bmatrix}\right) = \begin{bmatrix} n_6 \\ n_7 \\ n_8 \\ n_9 \end{bmatrix}$$

$$f\left(\begin{bmatrix} w_{1,10} & w_{2,10} & w_{3,10} & w_{4,10} & w_{5,10} \end{bmatrix} \cdot \begin{bmatrix} n_6 \\ n_7 \\ n_8 \\ n_9 \end{bmatrix} + [b_{10}]\right) = [n_{10}]$$

Where $w_{i,j}$ denotes the weight value of the connection between neurons n_i and n_j , and b_i denotes a bias to shift the output as needed. The activation function, $f(x)$, utilized to introduce non-linearity was the Rectified Linear Unit (ReLU) defined by

$$f(x) = \max(0, x)$$

Essentially, each neuron in one layer is an activation function applied to the sum of a weighted sum of each neuron in the preceding layer and a bias, with the first layer being the normalized attributes. This computation was done using Keras methods.

After the chlorophyll value was calculated (n_{10}), an inverse mapping was applied to remap the values to the chlorophyll-a concentration in $\mu\text{g/L}$. This was done through the utilization of methods in the Keras library as well.

Training

The training dataset was sourced from the National Centers for Environmental Information (NCEI) granule geoportal and the United States Geological Survey (USGS) water sample datasets and from NOAA. NCEI and USGS provided water quality data and NOAA provided UV index data. Data from the years 2014-2018 were used. [33,34] The UV index features had to be added through a Python program. The training dataset has 19596 data entries in total. The values in the dataset recorded for chlorophyll-a were shifted back by 5 days as immediate conditions do not accurately represent the immediate growth of algae [21]. In this way, our device is able to predict dangerous conditions in advance, and this method is valid for these attributes due to the high specific heat and physical properties of water in retaining conditions for long periods of time. After this shift, the data was normalized in code by computing the z score for each data point $(\text{input} - \text{mean})/\text{sqrt}(\text{variance})$. In this way, attributes with different ranges would not introduce unnecessary bias. The AntiBloom algorithm was optimized with gradient descent to minimize the cost function during neural network training. The cost function is computed as the square of the difference between the actual and predicted values. The standard training algorithm of backpropagation calculus is used to compute the gradient of the cost function to optimize each weight and bias ($w_{i,j}$, b_i) for cost minimization in the network. The training algorithm was executed using the Keras Python library.

Buoy Fabrication

A buoy was fabricated using a 3D printer and fiberglass. Half of the buoy developed with an original CAD design was printed in Polylactic Acid (PLA) and measured 5 in x 5 in x 3 in. Holes were drilled in the print to ensure that it could be removed from the fiberglass easily. Resin mixed with hardener was laid on two layers of fiberglass and cured overnight. The same procedure was repeated with the other half. Once the two halves were cured, the fiberglass was sanded down, and environmentally friendly acrylic latex paint was applied. A hole was drilled for the anemometer, Light emitting diode (LED) indicator, and UV wiring, which were connected to an Arduino and placed at the top. All circuitry was connected and tested for accuracy. An ArduCam was covered in epoxy to make it waterproof. A hole was drilled at the top for the ArduCam wire to be connected to the Arduino, and the ArduCam was placed at the top. All other wiring, including the Arduino and the Raspberry Pi 4, was placed inside the casing. Three holes were drilled on the bottom for each probe sensor (water temperature, pH, and salinity), and waterproof epoxy was added to protect the electronics inside the buoy. In order for the waterproofed buoy to remain upright, a container with a weight was attached to the bottom of the device with waterproof epoxy. At the end, a waterproof Quick Response (QR) code was added to the buoy facing any walking-by pedestrians. By appealing to intrinsic human curiosity, many will be intrigued by the QR code in the water and want to find out more. This link will direct them to a website we created that informs the general public on the purpose of our buoy, the harmful effects of algal blooms and water pollution, and what they individually can do to help the general public. As the goal of this buoy is to be utilized in local lakes and ponds across the globe, it will effectively create awareness and inspire the general public, hopefully leading to long-term improvement.



Figure 2. The AntiBloom device

Data Collection and AntiBloom Architecture

The buoy was placed in the desired body of water (Figure 2) to read data. The algorithm was run on the collected data to predict chlorophyll-a levels. If the chlorophyll-a levels were above $25\mu\text{g/L}$, the ArduCam was signaled to take a picture, upload it to an AWS S3 bucket, and return the image address to the Raspberry Pi. The threshold of $25\mu\text{g/L}$ was chosen as this falls in the range of moderate to high risk of algal bloom possibility as stated in literature [23]. All JavaScript Object Notation (JSON) files were uploaded to the AWS S3 Bucket. AWS Lambda was utilized to check each JSON file for an image address. If an image address was present, AWS SNS was used to send a notification of information regarding the JSON file to a desired party to request immediate action to prevent an incoming algal bloom. For testing purposes, a personal phone number was used as the selected party to receive the notification. This is to replicate the process of alerting local authorities, who, when

informed, can therefore take immediate action to impede the further growth of algal blooms (Figure 3). This will protect the marine life present in the water as well as local residents.

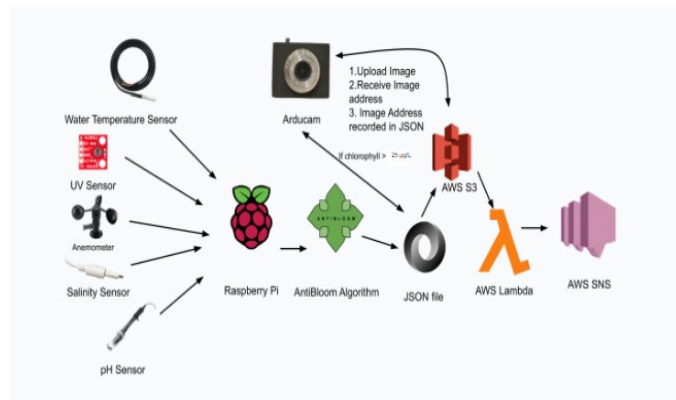


Figure 3. Model of the AntiBloom Architecture

Evaluating Metrics

K-fold cross-validation was used to determine the average accuracy of the algorithm through implementation with the Python SKlearn library. A k-value of 10 is used to ensure representative samples for reliable evaluation. The data is split into 10 subsets, where each subset is set at the validation set over 10 iterations. The algorithm is trained on all other subsets and checked against the validation set. The average accuracy of all 10 iterations is the final recorded accuracy of the algorithm. If the algorithm predicts an elevated level of chlorophyll and the data confirm that the level of chlorophyll is above $25\mu\text{L/g}$ the next day, it is deemed a correct prediction and a notification is sent. The algorithm predicts 5 days into the future as conditions correlate with algal growth after 5 days. We also calculated the final contribution weightings of each attribute to validate against the correlation heat map of the data set for chlorophyll-a. This process is repeated five times, running the program a total of 50 times, where the average percent contribution for each attribute is recorded as well.

Results

The data that was utilized to train the ANN model was taken from the NCEI granule portal and USGS water quality samples for Lake Erie. Through the use of a Python program, wind speed and UV index data were added from the OpenWeather API.

The InterQuartile Range (IQR), (Figure 4), represented by the height of the box, is 0.14%. The whiskers above and below the box represent the range of distributions. Any value less than $Q1 - (1.5 \cdot \text{IQR})$ or greater than $Q3 + (1.5 \cdot \text{IQR})$ was to be recorded as a point representing an outlier. The median accuracy is 96.34%. The range between the most accurate run and the least accurate run is 2.02%. The average accuracy is 96.1%.

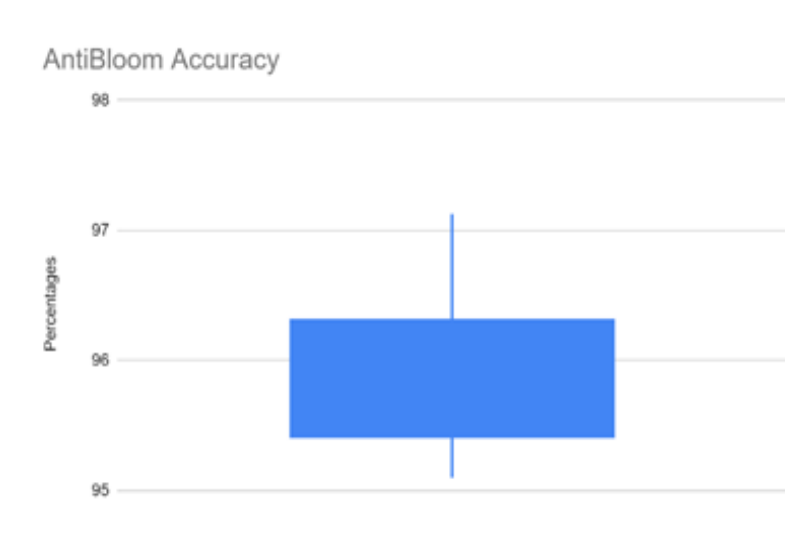


Figure 4. Displays a box plot of the distribution of percent accuracy after running the algorithm for 5 epochs utilizing k-fold cross-validation with a k-value of 10.

The correlation between the attributes and the target variable through the use of a heat map was determined (Figure 5). The radius and color of a circle are correlated to the degree of correlation of that attribute to Chlorophyll-a. UV has a Pearson's Correlation Coefficient of 0.46, wind speed has that of -0.01, water temperature has that of 0.04, pH has that of 0.14, and salinity has that of 0.26.

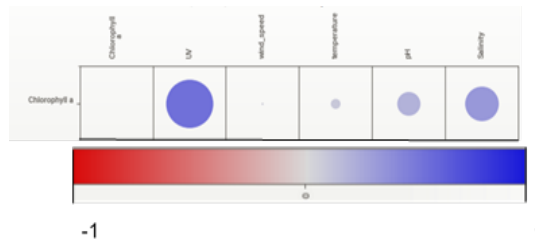


Figure 5. Heatmap of data created with Sweet Viz displaying the correlation for each attribute with Chlorophyll-a levels. The blue bar at the bottom shows the scale of the correlation (1 to 0).

In order to better understand the importance of each of our sensors in chlorophyll-a prediction, the percent contribution of each attribute was calculated (Figure 6). The x-axis shows the five trials conducted. The y-axis sums up to 100%, with each block in the stack proportional to the percentage that contributed to the final value. Over the 5 trials, the UV had an average contribution of 47.252%, salinity had 31.686%, pH had 15.112%, water temperature had 5.45%, and wind speed had 0.5%.

Discussion

ANN Model Effectiveness

The novel ANN model proved to have a median 96.34% accuracy in predicting chlorophyll-a concentration. The negligible range between the highest and lowest accuracy percentages of 2.02% proves the reliability and

consistency of the algorithm when predicting elevated levels of chlorophyll-a (Figure 4). In a similar study conducted by the members of the School of Electrical Engineering and Computer Science, it was found that the accuracy of their AI model was 91.0% when predicting chlorophyll-a levels for precision, not for classification [36]. The current results indicate that our device has a comparable level of accuracy in identifying dangerous conditions even with the use of less expensive sensors. Upon further analysis of the accuracy, it was observed that the model was making accurate predictions for both above and below the threshold value (25 $\mu\text{g/L}$). This high accuracy could partly be attributed to a relatively low sample size due to the limitations of the Raspberry Pi in regard to processing large amounts of data. This could mean the possibility of a Type 1 or Type 2 error. However, the standard of scaling the degrees of freedom or the number of parameters by 10 to estimate the minimum number of samples needed for a machine learning model was used. Therefore, we treat this accuracy with minimal concern for its validity.

Attribute Significance Analysis

The study demonstrates that a correlation exists between the attributes and levels of chlorophyll-a as from those alone, a high accuracy was obtained. This can be further corroborated by the correlation observed during both prior statistical analyses, with the UV index having a Pearson's correlation coefficient of 0.46, salinity having a coefficient of 0.26, and pH having a correlation of 0.14, and during the analysis of the percent contribution of the attributes to the final outcome, which displayed an order of significance similar to that of the magnitude of the Pearson's Correlation Coefficient (Figure 5 and Figure 6). The correlation here indicates that a focus on the more significant attributes, UV, pH, and salinity, can be considered in future research on algal bloom causation and prediction.

Conclusion

Overall, the attempt to create a low-cost device that is able to effectively predict algal blooms proved successful. The algorithm proved to be 96.34% accurate in chlorophyll-a prediction even while using low-cost sensors. The ability of the sensors was found to be highly accurate providing sufficient data to make precise predictions. 100% of the data was transferred to the AWS bucket, which also successfully sent a notification for any worrying predictions. Though strong, every design can always be improved. A problem acknowledged is the battery life of the Raspberry Pi, as a 9V battery was used. A possible way to do this is by utilizing a DFRobot Solar Power Manager to power the Arduino. It is a low-cost option that is compatible with non-lithium batteries, making it an eco-friendly option to keep the buoy in water for prolonged periods of time. In addition to this, a method called pruning can be utilized to remove unnecessary neurons from the AntiBlooms algorithm, further optimizing its performance. However, the combination of high accuracy, low cost, and communication effectiveness makes this buoy a perfect candidate for mass production and water quality monitoring in all bodies of water.

The future of AntiBloom lies in algal bloom prevention in local ponds and lakes across the globe. Through the use of its QR code, its message of better treatment of our local bodies of water is effectively spread. As for its next steps, research for AntiBloom does not need to be limited to just chlorophyll-a predictions. Due to its robustness and flexibility, AntiBloom has the capability to house, collect, and send data using other sensors for analysis. This could be used to detect nanoplastics and various toxic chemicals in local bodies of water when appropriate sensors are installed. With additions such as these, our AntiBloom device can be transformed into an optimal tool for water analysis, data collection, and notification.

Acknowledgments

We thank Mr. Zachary Kingman from Poolesville High School for allowing us to use the school 3D printer and training us on how to work with fiberglass and other materials to build our device. We thank Dr. Patricia Miller and the Science Montgomery Fair judges for providing feedback to elevate our project further. We also thank Brad Lovett, organizer of the Stockholm Junior Water Prize, as well as the judges who provided us with insightful comments.

References

- [1] Harvell CD, Kim K, Burkholder JM, Colwell RR, Epstein PR, Grimes DJ, Hofmann EE, Lipp EK, Osterhaus AD, Overstreet RM, Porter JW, Smith GW and Vasta GR (1999). Emerging marine diseases-- climate links and anthropogenic factors. *Science* 285, 1505-1510.
- [2] Bossart GD, Baden DG, Ewing RY, Roberts B and Wright SD (1998). Brevetoxicosis in manatees (*Trichechus manatus latirostris*) from 1996 epizootic: Gross, histologic, and immunohistochemical features. *Toxicol Pathol* 26, 276–282.
- [3] Backer LC, Fleming LE, Rowan A, Cheng YS, Benson JM, Pierce RH, Zaias J, Bean J, Bossart GD, Johnson D, Quimbo R and Baden DG (2003). Recreational exposure to aerosolized brevetoxins during Florida red tide events. *Harmful Algae* 2, 19–28.
- [4] Pierce RH, Henry MS, Blum PC, Lyons J, Cheng YS, Yazzie D and Zhou Y (2003). Brevetoxin Concentrations in marine aerosol: Human exposure levels during a *Karenia brevis* harmful algal bloom. *Bull Environ Contam* 70, 161–165.
- [5] Ye C, Shen Z, Zhang T, Fan M, Lei Y and Zhang J (2011). Long-term joint effect of nutrients and temperature increase on algal growth in Lake Taihu, China. *J Environ Sci (China)*. 2011; 23 (2): 222-7.
- [6] Davis TW, Berry DL, Boyer GL and Gobler CJ (2009). The effects of temperature and nutrients on the growth and dynamics of toxic and non-toxic strains of *Microcystis* during cyanobacteria blooms. *Harmful Algae* 8, 715-725.
- [7] Moe SJ, Couture RM, Haande S, Solheim AL and Jackson-Blake L (2019). Predicting lake quality for the next generation: Impacts of catchment management and climatic factors in a probabilistic model framework. *Water* 11, 1767-1791.
- [8] Paerl HW, Fulton RS, Moisaner PH and Dyble J (2001). Harmful freshwater algal blooms, with an emphasis on cyanobacteria. *Sci. World J.* 1, 76–113.
- [9] Havens KE, Philips EJ, Cichra MF and Li BL (1998). Light availability as a possible regulator of cyanobacteria species composition in a shallow subtropical lake. *Freshw. Biol.* 39, 547–556.
- [10] YANG X, WU X, HAO H and HE Z (2008). Mechanisms and assessment of water eutrophication. *J Zhejiang Univ Sci B* 9, 197-209.
- [11] Sunda WG, Graneli E and Gobler CJ (2006). Positive feedback and the development and persistence of ecosystem disruptive algal blooms. *J. Phycol.* 42, 963–974.
- [12] Sunda WG and Shertzer KW (2014). Positive feedbacks between bottom-up and top-down controls promote the formation and toxicity of ecosystem disruptive algal blooms: a modeling study. *Harmful Algae* 39, 342–356.
- [13] Kramer BJ, Davis TW, Meyer KA, Rosen BH, Goleski JA, Dick, GJ, Genesok Oh and Christopher JG (2018). Nitrogen limitation, toxin synthesis potential, and toxicity of cyanobacterial populations in Lake Okeechobee and the St. Lucie River Estuary, Florida, during the 2016 state of emergency event. *PLoS One* 13 (5).

- [14] Dodds WK, Bouska WW, Eitzmann JL, Pilger TJ, Pitts KL, Riley AJ, Schloesser JT and Thornbrugh DJ (2009). Eutrophication of U.S. Freshwaters: analysis of potential economic damages. *Environ. Sci. Technol* 43, 12–19.
- [15] Kudela RM (2015). Harmful algal blooms: A scientific summary for policy makers – UNESCO Digital Library. IOC/INF-1320 REV <https://unesdoc.unesco.org/ark:/48223/pf0000233419> (2015).
- [16] Kim HC and Yoo S (2007). Relationship between phytoplankton bloom and wind stress in the Japan/East Sea sub-polar frontal area. *J. Mar. Syst.* 67, 205–216.
- [17] Paul VJ (2007). Global warming and cyanobacterial harmful algal blooms. In: Hudnell, H.K. (ed.), *Cyanobacterial harmful algal blooms: State of the science and research needs*. *Adv. Exp. Med. Biol.* 619, 239–257.
- [18] Hallegraeff GM (2010). Ocean climate, phytoplankton community responses, and harmful algal blooms: A formidable predictive challenge. *J. Phycol.* 46, 220–235.
- [19] Fu FX, Tatters AO and Hutchins DA (2012). Global change and the future of harmful algal blooms in the ocean. *Mar. Ecol. Prog. Ser.* 470, 207–233.
- [20] O’Neil JM, Davis TW, Burford MA and Gobler CJ (2012). The rise of harmful cyanobacteria blooms: The potential roles of eutrophication and climate change. *Harmful Algae* 14, 313–334.
- [21] Humphries G, Magness DR and Huettmann F, Eds. (2018) *Machine Learning for Ecology and Sustainable Natural Resource Management*, Springer International Publishing, Cham 185-203.
- [22] Chorus I and Bartram J (1999). *Toxic cyanobacteria in water: A guide to their public health consequences, monitoring and management*. World Health Organization.
- [23] Yuan LL, Pollard AI, Pather S, Oliver JL and D’Anglada L (2014). Managing microcystin: Identifying national-scale thresholds for total nitrogen and chlorophyll a. *Freshwater Biol.* 59, 1970–1981.
- [24] McElhiney J and Lawton LA (2005). Detection of the cyanobacterial hepatotoxins microcystins. *Toxicol Appl Pharmacol.* 203, 219–230.
- [25] Zurawell RW, Chen H, Burke JM and Prepas EE (2005). Hepatotoxic cyanobacteria: a review of the biological importance of microcystins in freshwater environments. *J Toxicol Environ Health B Crit Rev.* 8, 1–37.
- [26] US EPA (2015). Drinking water health advisory for the cyanobacterial microcystin toxins. EPA-820-R-15100.
- [27] Abiodun OI, Jantan A, Omolara AE, Dada KV, Mohamed NA and Arshad H (2018). State-of-the-art in artificial neural network applications: A survey. *Heliyon.* 4, e00938.
- [28] Marzban C and Stumpf GA (1996). Neural Network for Tornado Prediction Based on Doppler Radar-Derived Attributes. *Journal of applied meteorology* (1988) 35, 617-626.
- [29] Safi Y and Bouroumi A (2013). Prediction of forest fires using Artificial neural networks. *Applied Mathematical Sciences* 7, 271-286.
- [30] Mellios N, Moe SJ and Laspidou C (2020). Machine learning approaches for predicting health risk of cyanobacterial blooms in northern european lakes, *Water* 12, 1191.
- [31] Medina JD, Arias A, Triana JM and Giraldo LF, Segura-Quijano F, Gonzalez-Mancera A, et al. (2022) Open-source low-cost design of a buoy for remote water quality monitoring in fish farming. *PLoS ONE* 17(6).
- [33] Cooperative Institute for Great Lakes Research, University of Michigan; NOAA Great Lakes Environmental Research Laboratory (2019). Physical, chemical, and biological water quality data collected from moored buoy WE02, Lake Erie in the Great Lakes region from 2014-05-22 to 2018-10-15 (NCEI Accession 0190201). NOAA National Centers for Environmental Information. Dataset. <https://www.ncei.noaa.gov/archive/accession/0190201>. Accessed January 21, 2023.
- [34] Index of /long/UV/cities. (n.d.). <https://ftp.cpc.ncep.noaa.gov/long/uv/cities/>

- Aquatic toxins.* Aquatic Toxins | Florida Department of Health. (n.d.). Retrieved April 15, 2023, from <https://www.floridahealth.gov/environmental-health/aquatic-toxins/>
- Backpropagation.* Brilliant Math & Science Wiki. (n.d.). Retrieved April 15, 2023, from <https://brilliant.org/wiki/backpropagation/#:~:text=Backpropagation%2C%20short%20for%20%22backward%20propagation,to%20the%20neural%20network's%20weights.>
- Centers for Disease Control and Prevention. (2022, May 2). *Illness and symptoms: Cyanobacteria in freshwater.* Centers for Disease Control and Prevention. Retrieved April 15, 2023, from <https://www.cdc.gov/habs/illness-symptoms-freshwater.html>
- Environmental Protection Agency. (n.d.). EPA. Retrieved April 15, 2023, from <https://www.epa.gov/nutrientpollution/effects-environment#:~:text=Algal%20blooms%20can%20reduce%20the,recreation%2C%20businesses%20and%20property%20values.>
- Niazkar, H. R., & Niazkar, M. (2020, November 23). *Application of artificial neural networks to predict the COVID-19 outbreak - global health research and policy.* BioMed Central. Retrieved April 15, 2023, from <https://ghrp.biomedcentral.com/articles/10.1186/s41256-020-00175-y>
- SheetalSharma. (2022, August 18). *Artificial Neural Network (ANN) in Machine Learning.* Data Science Central. Retrieved April 15, 2023, from <https://www.datasciencecentral.com/artificial-neural-network-ann-in-machine-learning/>
- U.S. Department of Health and Human Services. (n.d.). *Algal blooms.* National Institute of Environmental Health Sciences. Retrieved April 15, 2023, from <https://www.niehs.nih.gov/health/topics/agents/algal-blooms/index.cfm>
- Understanding algal blooms.* SJRWMD. (2022, October 6). Retrieved April 15, 2023, from <https://www.sjrwmd.com/education/algae/#gsc.tab=0>
- What is a harmful algal bloom?* National Oceanic and Atmospheric Administration. (n.d.). Retrieved April 15, 2023, from <https://www.noaa.gov/what-is-harmful-algal-bloom#:~:text=Harmful%20algal%20blooms%2C%20HABs,shellfish%20marine%20mammals%20and%20birds.>